Performance of pin-fin structures on pool boiling heat transfer

Falsetti, Chiara; Chetwynd-Chatwin, Jason; Walsh, Edmond J.

DOI
10.1016/j.ijft.2024.100784

Publication date
2024

Document Version
Final published version

Published in
International Journal of Thermofluids

International Journal of Thermofluids 23 (2024) 100784

Contents lists available at ScienceDirect

International Journal of Thermofluids

journal homepage: www.sciencedirect.com/journal/international-journal-of-thermofluids

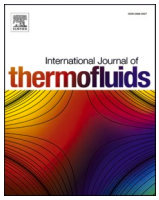

Performance of pin-fin structures on pool boiling heat transfer

Chiara Falsetti [a,1], Jason Chetwynd-Chatwin [b], Edmond J. Walsh [a,*]

[a] Thermofluids Institute, Department of Engineering Science, University of Oxford, Oxford, UK
[b] Rolls-Royce plc, Bristol, UK

ARTICLE INFO

Keywords:
Pool boiling
Heat transfer enhancement methods
Pin fins performance
CHF limit

ABSTRACT

The present study investigates pool boiling heat transfer of Novec 649 on structured copper surfaces. Structures with varying height and spacing, in the range of 400–1200 μm, were machined on the boiling surface using electro-discharge machining (EDM). Pool boiling experiments have been performed to estimate the heat transfer performance of pin-fin structures using Novec 649 as the cooling fluid. The heat transfer coefficient (HTC) and the critical heat flux (CHF) limit of the structured surfaces have been estimated and compared to those of the unstructured ones, both in the horizontal and vertical orientation. In this work, the effects of pin fin heights and spacing, with dimensions similar to the capillary length scale, on the heat transfer coefficient and critical heat flux limit are examined. The experimental results demonstrate that adding pin-fin structures significantly enhances boiling heat transfer. Specifically, the HTC and CHF increases by factors of up to 10 and 2.8, respectively, compared to the smooth surface. This enhancement is primarily driven by the wetted area increase due to the pin-fin structures. The HTC per unit wetted area was found to be independent of geometry during the early stage of nucleate boiling and only exhibited a weak dependence on geometry in the later stages. Notably, the HTC per unit wetted area deteriorates when the pin fin spacing is less than the capillary length scale.

1. Introduction

In recent years, both convective and nucleate boiling have been extensively investigated for the advanced cooling of high-power electronics [1–4], telecommunication equipment [5], nuclear reactors [6] and fuel cells [7]. To assess the heat removal efficacy of a boiling system, the HTC and the CHF are crucial metrics. The HTC measures the heat removal capacity of the flow at a given temperature difference, while the CHF represents the key operational limit in most boiling systems. Upon reaching the CHF, a vapor film forms over the heated surface, causing a rapid increase in surface temperature, which typically leads to failure of device.

Active and passive techniques have been used to enhance the HTC and extend the CHF limit [8]. To date, among the many passive methods used, surface modifications enhance the thermal performance by changing wettability and increasing wetted area, as reviewed by Chua et al. [9]. A comprehensive review of microscale enhancement technique, including micro-fins, micro-channels, and porous coatings, was conducted by Liang and Mudawar [8]. The review underlines that machining micro-structures on the boiling surface increases both the nucleation sites and the surface area and, depending on the structure and dimension of the structures, they suggest that it might also promote liquid replenishment by capillary effect. In addition, patterning the surface could help in creating two separate paths where the vapor bubbles can rise, and the cold liquid move towards the boiling surface. These effects have led to improved boiling HTC and CHF for several designs [8,10]. However, as underlined by these reviews, a larger database for the microstructure enhancement methods using different fluids (especially non-aqueous fluids with low global warming potential), materials and machining techniques is needed for future applications of two-phase immersion cooling systems.

The performance of copper structured surfaces consisting of an array of squared fins have been tested by Guglielmini et al. [11] with Galden HT55 as working fluid. Their samples had a fixed fins height of 3 mm and two different spacings of 0.4 mm and 0.8 mm, respectively. The samples with smaller spacing between fins showed a slightly higher heat transfer performance, due to a larger number of active nucleation sites. This performance increase was not proportional to the larger boiling area given by the smaller spacing between fins. They concluded that when the spacing is smaller than the bubble departure diameter, calculated with the properties of the selected fluid, the structures

* Corresponding author.
E-mail address: edmond.walsh@eng.ox.ac.uk (E.J. Walsh).
[1] Current affiliation: Propulsion and Power, Delft University of Technology, Delft, NL

https://doi.org/10.1016/j.ijft.2024.100784

Available online 30 July 2024

Nomenclature

cp	specific heat, J/kgK
Db	bubble departure diameter, m
CHF	critical heat flux, W/cm^2
g	gravity m/s^2
GWP	global warming potential
HTC	heat transfer coefficient, W/m^{2}K
h_{fg}	latent heat of vaporization, J/kg
k	thermal conductivity, W/mK
L	length of the heat sink, m
L_c	capillary length
M	molecular weight, g/mol
p	Pressure, bar
Pr	Prandtl number
q''	Heat flux, W/m^2
R_a	average surface roughness, μm
R	surface area ratio
T	Temperature, K
ΔT	Excess temperature, K
u	velocity, m/s
x	position, m

Greek symbols

α	thermal diffusivity, m^2/s
η	fins efficiency
ρ	density kg/m^3
σ	surface tension, N/m
μ	dynamic viscosity, Pa s
υ	kinematic viscosity, m^2/s

Subscripts

exp	experimental
centr	central
corr	correlation
ftp	footprint
l	liquid
r	reduced
sat	saturation
v	vapor
w	wall
WA	wetted area
Tot	total

interfere with the bubble departure.

Rainey and You [12] performed boiling experiments with FC-72 and compared a plain and structured surfaces with squared fins. The pin fins height varied from 0 to 8 mm, and the spacing was of 1 mm. The boiling curves of the different structured samples are similar at low heat fluxes. The height starts to have an effect at higher heat fluxes, close to CHF. They estimated the temperature at the fin tips and showed that for the longer fins the temperature was not enough to start nucleation. Moreover, they showed that the tallest fins impacted the bubble departure and delayed rewetting. For these effects, they found an optimal fin height of around 5 mm. Looking at the microporous covered fins, the estimated excess temperature at the tips just before CHF was around 19 K, well over the superheat required for nucleate boiling allowing high heat transfer coefficients over the whole fin.

The effects of fins height and spacing on pool boiling heat transfer of FC-72 have been studied by Yu and Lu [13]. The fins were made in copper with spacings of 0.5 mm, 1 mm, and 2 mm and heights of 0.5 mm, 1 mm, 2 mm, and 4 mm. For the largest spacing, boiling curves were similar at low heat fluxes until values close to the CHF limit, where the tallest fins outperformed the others. At lower spacing, the boiling curves were not similar among samples, and the shortest fins showed a higher performance at lower heat fluxes, despite the smaller boiling area, while the tallest structures were performing better at high heat fluxes. Their results showed that the highest performance was achieved by the tallest and most closely spaced pin fins, resulting in a CHF five times larger than the plain surface. The flow visualisation results from Yu and Lu [13] confirmed what previously observed by Rainey and You [12]. Using a high-speed camera, they observed that when the spacing reduces, the boiling curves depend on the structure's height, even at low heat flux values and that bubble coalesce occurs more rapidly.

Water pool boiling experiments were conducted by Zou and Maroo [14], who reported a CHF enhancement of 2.25X by fabricating nano/micro ridges on the surfaces and enhancing the surface area by 40 %. The CHF enhancement was found only when the ridge heights were below a critical threshold, which was the thickness of the non-evaporating film (of 450 nm and 900 nm for Si and SiO2 surfaces, respectively).

Kim et al. [15] studied pool boiling of deionised water using micro-structured surfaces. They designed a range of cylindrical micro-structures varying heigh, diameter, and gap in the range of 0–40 μm. They defined the "non-dimensional roughness" as the ratio of the surface area with micro-fins to the smooth area and quantified its effect on water boiling performance. They showed that the HTC and the CHF were enhanced by up to 3X and 3.5X, respectively with the addition of micro-fins. They indicated an optimal gap size for the CHF enhancement, as the CHF was higher for 20 μm than 40 μm gap, showing that when the gap is larger than a critical value, the inflow of cold liquid to the heated wall gradually decreased due to reduced capillary pressure.

Boiling enhancement of water on copper structured surfaces was investigated by Rahman and McCarthy [16]. They tested microchannels and nanostructured coatings. They showed that microstructures on the order of 300–400 μm increased nucleation and bubble dynamics at low fluxes, enhancing the CHF of 2X and HTC up to 4.5X compared with smooth copper surface. Nano-coatings only produced an increase in CHF by capillary wicking, with no enhancement in the HTC.

Boiling of Novec 649 was studied by Kaniowsky [17], who compared smooth copper samples with microchannels ones. The microchannels width was 300 μm, the spacing was 100 μm and the depth varied of 200–300–400 μm. The channels with depth of 300 microns gave the best heat transfer results, with an increase in the HTC of 3.5 times compared to the smooth sample (max HTC 7.6 kW/m^{2}Kversus 2.3 kW/m^{2}K). At atmospheric pressure conditions, the CHF improved from ~7.5 W/cm^2 at a superheat of ~35–38 K to a value of ~11W/cm^2 at ~15–18 K. Gouda et al. [18] experimentally investigated pool boiling heat transfer of deionised water using copper segmented finned and uniform cross-section micro-channels structured surfaces. The cross-section of microchannel was of 400 μm and 450 μm in width and depth, and fin width was 200 μm. The surface area was increased 2.5 times compared to the smooth surface. Their results indicated a 3X increase in HTC and a 1.6X increase in CHF for the structured surfaces compared to the plain surface. Pastuszko et al. [19] carried out experiments with water, Novec 649, ethanol and FC-72 and compared micro-fins structures with and without a porous coating, consisting of a sintered copper perforated foil with pores in the order of 100 μm. For the same test section with fin structures of 1000 μm height, 2000 μm width and a gap between structures of 600 μm, the highest HTC found for Novec 649 was ~5 kW/m^{2K} while for FC-72 and ethanol was of ~10 kW/m^{2K} and ~20 kW/m^{2K} The reported CHF was of ~15 W/cm^2, ~20 W/cm^2 and ~33 W/cm^2 for Novec 649, FC-72 and ethanol, respectively. In a more recent study, the same authors used their experimental data with Novec 649 to

develop a model to predict heat fluxes with micro-channels surfaces. The proposed model mechanistic model estimates the heat fluxes with $a \pm$ 35 % error [20].

Cao et al. [21] studied the pool boiling performance of Novec 649 on copper surface with microporous structures fabricated by electro-chemical deposition. The microporous structures consist of a pattern of micro-pores, nano-cavities, and irregular dendrites. The porosity varied between 40 % to 60 %, the roughness Ra from 10.9 μm to 17 μm, and the increase of surface area compared to the smooth sample was varying between 1.91 to 2.03 times. When comparing the coated samples with the smooth one (having Ra of 0.094 μm) they obtained an enhancement of 5.8 times in the HTC (from 4 $kW/m^{2K}$to 35 kW/m^{2K})and of 1.53 times in CHF (from 17 W/cm^2 to 26 W/cm^2). In a following study, the authors tested new surfaces with micro- and nano-coatings with Novec 649, that achieved maximum heat transfer enhancement of 60 % and 460 %, respectively [22].

Pool boiling of FC-72 with cylindrical micro-structures of diameter varying from 25 to 255 μm etched in a silicon substrate was studied by Lei et al. [23]. The structures delayed CHF, showing an increase of 1.69 times that of the smooth sample with no subcooling. When the sub-cooling was increased to 35 K, the CHF of the structured surface becomes 2.02 times higher than the smooth one. They also observed a decrease in HTC at higher heat fluxes due a strong generation and combination of bubbles that induce a partial cover of the vapor on the boiling surface. They found that the distance between the patterns had a strong effect on the overall heat transfer enhancement and on the CHF increase.

Može et al. compared pool boiling of water, Novec 649 and water/butanol mixture using copper structured surfaces [24]. The surface with lower contact angle showed the highest CHF value, while the nano-structured one enabled enhanced rewetting. The study also investigate the aging effect using Novec 649, as repeatability of the results could not be verified.

Tang et al. [25] used electro-discharge machining with ad-hoc shaped wavy electrodes to develop micro pillars 450 μm wide, 220 μm high and spaced 550 μm on copper substrates of 10 mm x 10 mm. The fluid was deionised water. A maximum increase in CHF and HTC of 2.34 times and 1.8 times higher, respectively, have been obtained with the best performing microstructure sample when compared to the smooth surfaces. Additionally, the excess temperature for the onset of boiling was found to be 62 % lower with the microstructures compared with smooth surfaces.

More recently, pool boiling heat transfer of Novec 649 was studied with smooth and sandblasted copper surfaces by Falsetti et al. [26]. These studies reported a 3X increase in the heat, respectively, due to a higher number of active nucleation sites. The increased roughness of the sandblasted surfaces also promoted a higher CHF limit, of 1.5X [26].

The influence of bubble-fin interactions for optimising fins height and spacing with water and HFE-7100 has been studied by Winter and Weibel [27]. Copper fins were additively manufactured on a 20 mm x 20 mm boiling surface. The thickness of the fins was 1 mm, height and spacing varied from 0.5 mm to 8.5 mm. The study suggested that the fluid capillary length is the key length scale at which the effects of the fin height and confinement play a role. When the spacing is below the capillary length, the boiling curves strongly depend on the spacing, as there is confinement of vapor between fins. They found that if the fins height is below the capillary length, the CHF is nearly the same as the flat surface without structures. Having fins longer than the capillary length allows a stable film to form at the base of the fins, leading to an increase of the CHF limit of up to 4 times than the smooth surface. Indeed, they observed a CHF of ~101 W/cm^2 for the fins 8.5 mm tall, compared to a CHF of ~23 W/cm^2 for the smooth sample without fins.

It can be summarised that several pool-boiling studies on functionalised surfaces have used water as the heat transfer fluid, while only a few studies have utilised dielectric fluids, predominantly FC-72. Since boiling and bubble dynamics are highly dependent on the thermo-physical properties of the fluid, different behaviours have been observed between water and dielectric fluids in heat transfer with structured surfaces [28].

This paper investigates boiling heat transfer of the dielectric fluid Novec 649 on structured copper surfaces with square pin fins. Experimental surfaces are manufactured using the wire-EDM technique. The spacing and height of the pin fins are in the range of 400–1200 μm which spans the capillary length scale of Novec 649. The main conclusions are that wire-EDM manufactured surfaces with Novec 649 perform very well compared to the augmented surfaces in the recent literature surveyed. The HTC per unit wetted area is found to deteriorate when the pin fin spacing is less than the capillary length scale. However, it is important to note that even with a reducing HTC per unit wetted area, the overall thermal resistance of the surface improves as the increased number of pin fins with reduced spacing more than compensates for the reduction in HTC.

2. Experimental facility

The pool boiling facility consists of a polycarbonate cylinder that contains the test section and the working fluid. The cylinder has an inner diameter of 150 mm and height of 184 mm, and it has a stainless-steel base and an aluminum top lid. The liquid temperature of the pool is measured by two K-type thermocouples and the vapor pressure is measured by an absolute pressure transducer. The liquid saturation temperature is maintained by an auxiliary heater submerged in the pool. The cylinder is sealed by a silicon O-ring at the top and bottom plates and epoxy around the ports. An Alphacool NexXxos radiator is installed as the condenser on the aluminium top and connected to a temperature controlled (Lauda bath) water loop. By adjusting the water temperature in the condenser side, saturation pressure and temperature can be controlled. A schematic of the pool boiling experimental set-up, with view of the test section and structures, is depicted in Fig. 1.

The 3 M fluid Novec 649 has been chosen as heat transfer fluid, as it is dielectric and non-toxic, and it has a low global warming potential (GWP) of 1, i.e. the same impact per equal mass of CO_2. Its thermo-physical properties at pressure of 1 bar are outlined in Table 1.

The test sections are made in copper, with a bottom area of 51 mm x 51 mm, thickness of 5 mm, and the top boiling surface of 20 mm x 20 mm and thickness of 12 mm. Four thermocouples are installed 3 mm apart, and the top one is 1.5 mm below the boiling surface. These details are also highlighted in Fig. 1. An OMEGA self-adhesive polyimide flexible heater is glued to the bottom to generate the desired heat flux. The heater is rated up to 115 V, and it can withstand a maximum temperature of 150 °C.

In this study, surfaces with different finish and micro-structures have been tested and compared. The smooth surface, referred to as "SR1" sample, has a polished surface with an average surface roughness Ra of 0.1 μm measured by an optical profiler (μSurf Nanofocus). The pin-fin structures have been machined via electro-discharge machining (EDM). These samples will be referred to "SM" in the study. Moreover, when electro-discharge machining is used on the copper surface, the free surface of the channels between micro-structures is also modified and its roughness enhanced. As a control, a surface was created where the top layer was completely removed using EDM leaving a structure free surface. This test section has an average surface roughness Ra of 3.1 μm, and it will be referred to as "EDM". SEM images of the SR1, EDM and one SM surfaces are shown in Fig. 2. The microstructures in the SEM images are of width, height and spacing equal to 400 μm, corresponding to the sample SM2, see Fig. 2. The sizes of the microstructures have been measured using SEM images and ImageJ software. The measurement uncertainty was on the order of 5 μm on the 400 μm sample. A maximum deviation of 2 % from the nominal dimensions has been measured considering all samples.

The size of the microstructures and the gap between them have been selected to be on the order of the capillary length, calculated as:

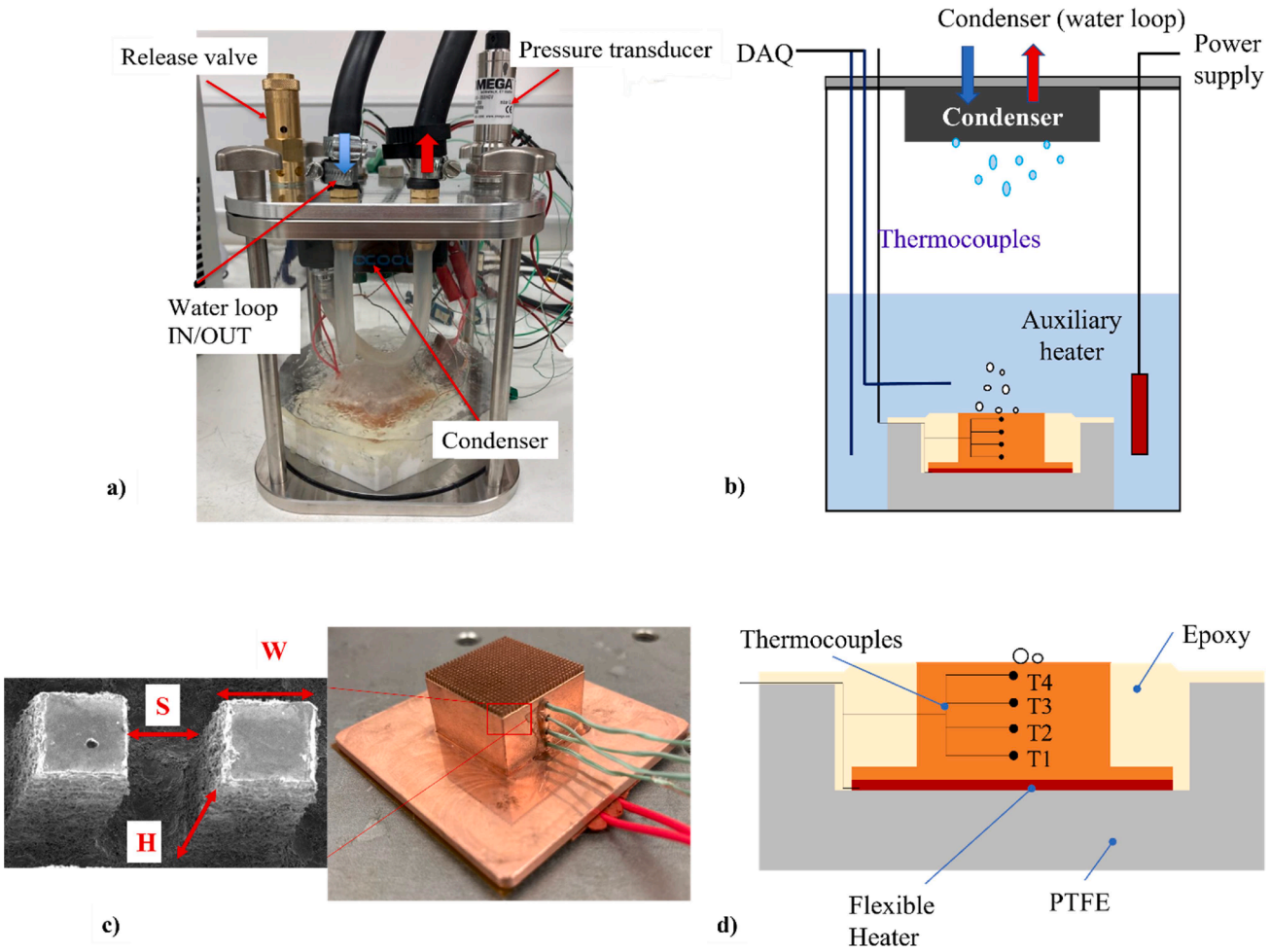

Fig. 1. (a) Picture and (b) schematic of the pool boiling setup. Picture (c) and schematic (d) of the test section with zoom on the pin-fin structures, machined on the boiling surface with EDM.

Table 1
Thermophysical properties of Novec 649 at pressure of 1 bar, saturation temperature 49 °C. Data from REFPROP NIST.

	$\rho_l\left[\frac{kg}{m^3}\right]$	$\rho_v\left[\frac{kg}{m^3}\right]$	$\sigma\left[\frac{N}{m}\right]$	$h_{lv}\left[\frac{J}{kg}\right]$	μ_l[Pa · s]	Pr_l[−]	M [g/mol]
Novec 649	1.5254e+03	12.9806	0.0089	8.7806e+04	4.8494e-04	10.09	316

$$L_c \propto \sqrt{\frac{\gamma}{(\rho_l - \rho_v)g}} \tag{1}$$

Using the thermophysical properties of Novec 649 at saturation conditions at 1 bar pressure, as indicated in Table 1, the capillary length is of 0.75 mm. When the height and spacing of the fins are larger than the capillary length, it has been shown that the fins in an array follow the boiling behaviour of a flat surface, i.e. the way the heat transfer coefficient varies with the surface superheat is the same [27]. To investigate this further, the height of the microstructures ("H") and the spacing between two adjacent pins ("S"), have been varied from 400 μm to 1200 μm. The sizes of the different microstructure samples, referred to as "SM" samples, the smooth "SR1", and the "EDM" samples are outlined in Table 2. The nominal surface ratio, R, calculated with the nominal dimensions of the fins with a perfect perpendicular shape is also indicated in Table 2.

However, the EDM machining process creates curved segments on the heat sink base between fins which increase the total area of the boiling surface, as it is possible to see from the SEM image at 30° inclination of Fig. 2. The relative surface area increase for the structured samples are calculated by assuming segments to have semi-circular profiles with a diameter equal to the spacing between the fins. The relative area ratio generated by the EDM machining is referred to as R_{EDM} in Table 2.

3. Data reduction and uncertainty analysis

In order to calculate the heat flux at the boiling surface, the 1D spatial temperature gradient in the copper test section along the vertical direction, $\frac{dT}{dx}$, is obtained by linearly interpolation of four thermocouple measurements. The heat flux through the upper surface is then calculated by Fourier's law and it is referred to as footprint heat flux:

$$q''_{ftp} = -k\frac{dT}{dx} \tag{2}$$

Since the copper sample is insulated on the lateral sides, it is possible to assume a 1D conduction. The distance between two adjacent thermocouples is dx. The thermal conductivity of the copper sample is $k = 390\frac{W}{mK}$. With the footprint heat flux, it is possible to calculate the

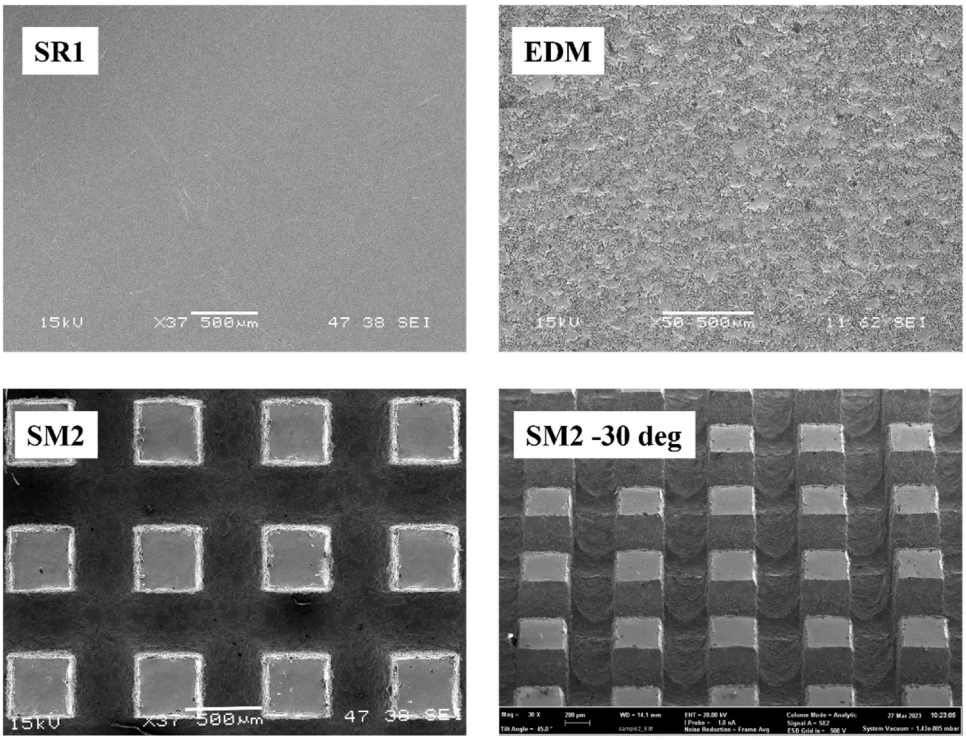

Fig. 2. SEM images of the smooth sample (SR1, Ra 0.1 μm), the EDM surface (Ra 3.1 μm) and the structured sample (SM2). Scale of the SEM images is 500 μm.

Table 2
Microstructures dimensions: W, H, S indicate the width, height and spacing of the pin fins Data from samples SM1 and SM3 have not been included in this study, due to problems with leakage and pressure regulation occurred during testing of those two samples.

Sample	Width, W [μm]	Height, H [μm]	Spacing, S [μm]	Surface ratio R [-]	EDM surface ratio, R_{EDM} [-]	Surface type / machining
SR1	–	–	–	1	1	Ra 0.1 μm/ CNC
EDM	–	–	–	1	1	Ra 3.1 μm / EDM
SM2	400	400	400	2	2.18	Microstructures / EDM
SM4	400	800	400	3	3.18	Microstructures / EDM
SM5	400	1200	400	4	4.18	Microstructures / EDM
SM6	400	400	800	1.5	1.85	Microstructures / EDM
SM7	400	400	1200	1.25	1.73	Microstructures / EDM

temperature of the boiling surface, T_w, as follows:

$$T_w = T_4 - \frac{q''_{ftp} \cdot \Delta x}{k} \tag{3}$$

Where T_4 is the uppermost temperature measurement, which is 1.5 mm (Δx) below the boiling surface. The excess temperature is the difference between the top surface temperature and the saturation temperature of the coolant kept at 1 bar inside the vessel, as $\Delta T = T_w - T_{sat}$. The saturation temperature value, T_{sat}, is also measured and double-checked by averaging the two thermocouple measurements in the liquid pool. The CHF limit is defined in terms of footprint area, when dry out occurs and the temperature of the boiling surface starts to increase rapidly.

The HTC based on footprint area is calculated using:

$$htc_{ftp} = \frac{q''_{ftp}}{T_w - T_{sat}} \tag{4}$$

To find the HTC based on total surface we determined the wetted surface area subject to nucleate boiling and the fin efficiency. With these variables the total surface efficiency can be found by addition of the unfinned surface area (assuming this has 100 % efficiency) and the surface area of the fins with the calculated fin efficiency as:

$$\eta_{total} = \left(1 - \frac{A_{fins}}{A_{total}}\right) + \frac{A_{fins}}{A_{total}} \eta_{fins} \tag{5}$$

$$\eta_{fins} = tanh(mL)/mL$$
$$mL = \left(\frac{hP}{kAc}\right)^{1/2} L \tag{6}$$

The fin efficiency, η_{fins}, is calculated assuming the fins tip to be adiabatic and using the averaged heat transfer coefficient based on surface area increase, i.e. $h = HTC_{ftp}/R$ in Eq. (6) [29].

The use of a single averaged heat transfer coefficient over the full height of the fin, while simplified, is reasonable as the maximum temperature difference between base and fin tip is <1 °C for all our test cases. The assumption of adiabatic tip is used since on the smooth surfaces (not EDM machined) of the fins tip as the heat transfer coefficient is over an order of magnitude less than for the EDM machined surfaces. Hence the averaged heat flux for the real wetted surface area is given by:

$$q''_{WA} = q''_{ftp} \Big/ R_{EDM} = \eta_{total} HTC_{WA} \left(T_{surf} - T_{sat}\right) \tag{7}$$

The subscript 'WA' indicates the wetted area minus fin tips. These calculations do not account for the increased surface area due to local surface roughness, however they are appropriate for comparison between samples with the same surface finish such as those made using the same manufacturing techniques, i.e. SM2 – 7.

The uncertainties of the measured and calculated quantities are given in Table 3. The uncertainty of the K-type thermocouples, installed

Table 3
Uncertainty values of the parameters of interest.

Variable	Instrument	Uncertainty
Liquid and copper temperature, T_{sat}, T_{1-4}	K-Type thermocouple	$0.2°C$
Vapor pressure, p_v	Absolute pressure transducer	0.08 % $\pm$ $0.2kPa$
Thermal conductivity, k	Manufacturer	1 % $3.9\frac{W}{K \cdot m}$
Positioning, x	Measured	0.2 mm
Heat flux, q''_{ftp}	Calculated (Eq. (2))	[4.8–11.4]%
Wall Temperature, T_w	Calculated (Eq. (3))	$0.34°C$
Superheat, $T_w - T_{sat}$	K-Type thermocouple	$0.39°C$
HTC	Calculated (Eq. (4))	[5–12.1]%

in the copper block and merged in the coolant, is obtained from the calibration performed in the LAUDA water bath over the temperature range of 50–90 °C, and it is measured to be of $0.2°C$. The uncertainties of the heat flux and the HTC are obtained by the propagation method proposed by Kline and McClintock [30]. The heat flux uncertainty includes the uncertainty of the linear regression used to obtain $\frac{dT}{dx}$.

The measurement procedure started by first cleaning the test specimens using an ultrasonic bath to remove any residue from the machining. Before the boiling experiments NOVEC 649 was poured in the pressure chamber with a liquid height of approximately 90 mm. The fluid was degassed for ~40 min by boiling and venting to the atmosphere. During experiments the vent is sealed, and the heat flux varied using the voltage of the power supply connected to the resistance heater. Each tested heat flux was given approximately ~1 h to reach steady state defined as less than 0.2 °C for a period of 5 min, before measurements were taken,. Each boiling curve took approximately one full day of testing.

To ensure repeatability and reliability of the experimental set-up, pool boiling experiments were repeated on different days using samples SM2 and EDM. The results indicate good repeatability between tests, as shown in the boiling curves illustrated in Fig. 3.

4. Results and discussion

4.1. Heat transfer performance of the smooth and structured surfaces

The effect of varying the fin spacing (S) and height (H) on boiling heat transfer is investigated and presented in this section. The size, dimensions and abbreviations of each sample are provided in Table 2.

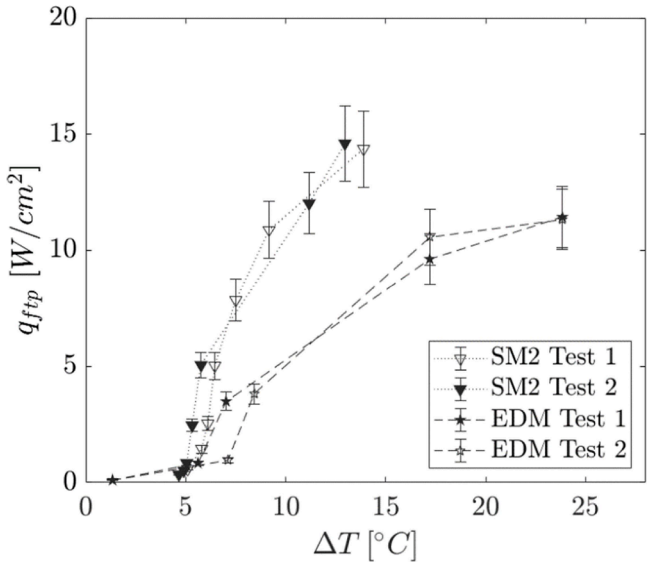

Fig. 3. Repeatability of the tests using the samples EDM and SM2. The results have been obtained from experiments repeated on different days.

Boiling curves for the structured samples with varying height (samples SM2–5), and those relative to the samples with varying spacing (SM2, SM6 and SM7) are shown in Fig. 4(a)-(b), respectively. The boiling curves of the smooth (SR1) and EDM samples are also plotted for comparison. The heat flux is calculated based on the footprint area, which is equal to 20 × 20 mm^2 for all samples, and the excess temperature is calculated with the wall and saturation temperatures, as explained in the data reduction section.

The results show that the structured samples outperform the SR1 and EDM samples over the whole range of tested heat fluxes, thanks to a larger surface area and more active nucleation sites.

The curves are shifted towards lower excess temperatures for same heat flux when compared to the surfaces without micro-structures. The onset of boiling is reduced from ~22 K to ~5 K, and it is similar for all structured samples. The heat transfer in the nucleating bubble regime grows very rapidly at increasing heat fluxes. For example, at a constant heat flux value of 10 W/cm^2, the excess temperature reduces from ~40 K to 5 K, which results in a reduction in the wall temperature from ~90 °C to ~55 °C. From an application perspective, this enables electronic devices to operate at lower junction temperatures, or at higher power densities. The EDM surface shows a heat transfer improvement when compared to the smooth sample SR1, likely due to the higher number of active nucleation sites generated by a surface roughness 30 times higher (R_a of 3.1 μm vs 0.1 μm). Also, the CHF limit is increased from 13.6 W/cm^2 to 16.5 W/cm^2 when comparing the SR1 and EDM surfaces.

A summary of the CHF and maximum footprint heat transfer coefficient values of the tested samples is outlined in Table 4 and Fig. 5. The results of Fig. 5 shows the variation of the maximum footprint HTC and the CHF with the height (H) and spacing (S) between fins. As it is possible to observe in Fig. 5(a), both the HTC and CHF increases in a quasi-linear fashion with the structure's height, as the heat transfer area increases. The highest CHF and footprint HTC have been found for the sample SM5, which presents the tallest pin fins and the highest surface area increase.

Among the three samples with same pin fin geometry but different spacing (SM2-SM6 and SM7), the highest CHF value of 23 W/cm^2 has been found for the sample SM6, with spacing matching the capillary length, $S = 800$ μm. Despite SM2 having the highest nominal heat transfer area compared to SM6 and SM7, (x2 versus x1.5 and x1.25), it presents the lowest CHF value. This result suggests that the nominal increase of surface area is not the only parameter impacting the CHF limit in structured surfaces, and therefore not the only one to consider in the design of heat sinks for immersion cooling applications, in agreement with a recent study using FC-72 as coolant [31].

As indicated by these results, finned surfaces and the machining technique impact on the surface enhance the CHF limit, that is up to 3 times as large as that for the smooth surface.

The CHF calculated with Zuber correlation [32], using a value of $\pi/24$for the constant and the thermophysical properties of Novec 649 at 1 bar pressure, is equal to 14 W/cm^2. This predicted value is very close to the experimental value found for the smooth sample SR1 of 13.6 W/cm^2 (see *Table 4*). While Zuber correlation predicts the CHF for unstructured surfaces accurately, it is not adequate to estimate the CHF when pin-fin structures are machined on the boiling surface.

The results of four other studies using Novec 640 on different treated copper surfaces [20–22,24], are considered, although a direct comparison is difficult comparing key parameters of CHF and HTC is informative regarding the relative performance of wire-EDM machining. In both studies by Cao et al. [21,22], the smooth sample had a roughness of 0.094 μm, with HTC and CHF within 10 % of the EDM surface in this study. Their best micro-particle coated surface, prepared via electrochemical deposition, had a footprint CHF of ~27 W/cm^2, ~40 % less than sample SM5 herein. There nanoparticle-coated surfaces exhibited the best HTC value peaking at ~2.11 W/cm^{2K} [22].

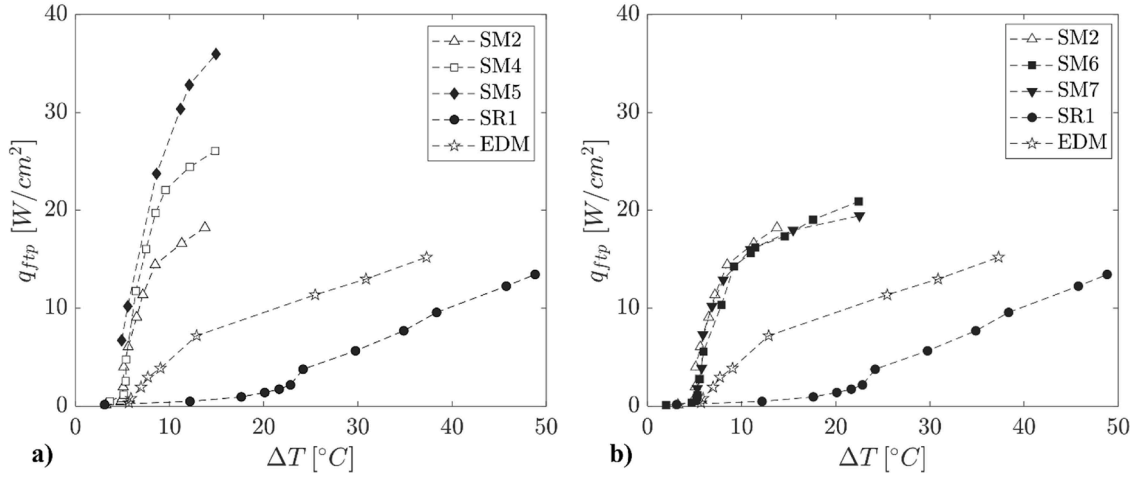

Fig. 4. Boiling curves for pin-fin structured samples. The samples with (a) different height and (b) spacing are compared to the smooth and EDM samples. The heat flux is calculated based on the footprint area.

Table 4
Summary of CHF values and maximum footprint HTC for the samples tested in this study.

Sample	CHF [W/cm^2]	Max HTC_{ftp} [W/cm^{2}K]
SR1	13.6	0.27
EDM	16.5	0.55
SM2	20.4	1.70
SM4	26.9	2.31
SM5	39	2.75
SM6	23	1.55
SM7	21.1	1.60

Kaniowski et al. [20] tested a copper surface with microchannels (400 μm width and 200–500 μm height), and found a maximum HTC of 2.23 W/cm^{2K}. The CHFs were comparable to those in the present study, ranging from 19.5 W/cm^2 to 27.8 W/cm^2 from shortest to tallest channels. Finally, the present data were compared to Moze et al. [24], who observed a significant overheat effect at the onset of boiling (approximately 8–10 K), which was not observed in our study. The maximum CHF value of their structured surface (Type B) was 24 W/cm^2 and the maximum heat transfer coefficient was found to be approximately 1.5 times lower than that of SM5.

4.2. Fin efficiency and heat transfer performance

In order to compare the different pin-fin structures and evaluate the impact of surface area increase on heat transfer, an analysis using fin efficiency is performed. The data presented in this section are obtained by dividing the footprint heat transfer coefficient, HTC_{ftp}, by the fin efficiency, η_{fins}, and by the EDM surface area increase, R_{EDM} (see Table 2). This ratio, referred to as HTC_{WA}, is presented as a function of excess temperature and heat flux in Figs. 6 and 7 respectively.

As shown the different heat transfer coefficient curves collapse in the early nucleate boiling region until a value of $HTC_{WA} \sim 0.5$ W/cm^{2}K.

This suggests that the heat transfer coefficient for fins up to 1200 μm tall is not significantly impacted by the effect of bubble confinement in the early stages of nucleate boiling where the bubble size is still small. The reduction in the maximum heat transfer coefficient with increasing fins height is less than 20 %, while the height increased of three-fold. This reduction likely due to larger bubbles in the latter stages of nucleate boiling impeding the fluid returning to the hot surface. It is noted that all fin efficiencies were > 92 % (SM5 with the tallest fins had an efficiency of 92.4 %), resulting in the lowest surface efficiencies of > 94 %. This hypothesis is further supported since with increasing fin spacing (from SM2 to SM6 to SM7) bubbles are no longer restricted and the maximum HTC increases as shown in Fig. 6. For completeness, the data is replotted in Fig. 7 against heat flux of the wetted surface heat

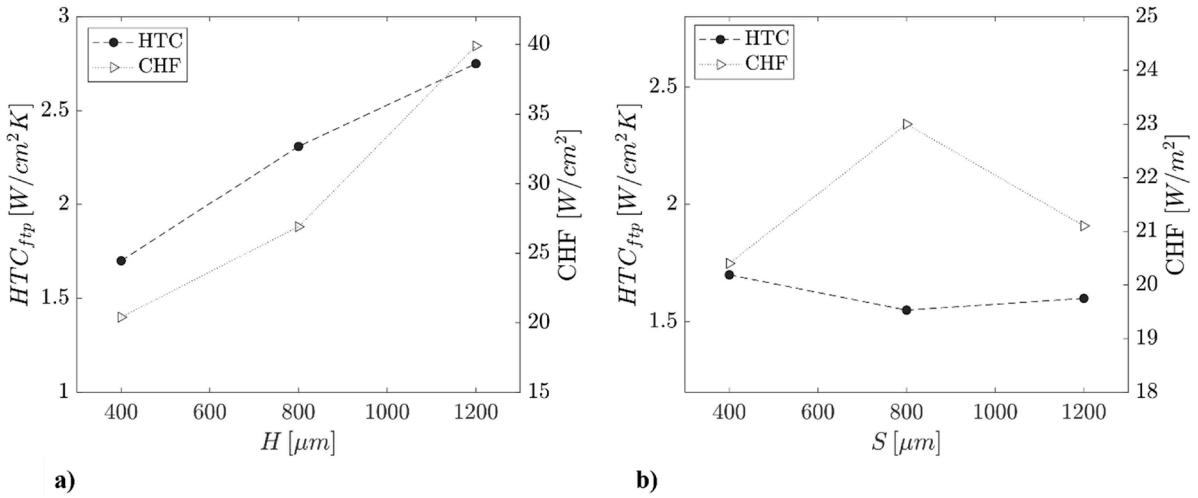

Fig. 5. Maximum HTC and CHF when varying (a) height H, and (b) spacing S of the pin-fin structures.

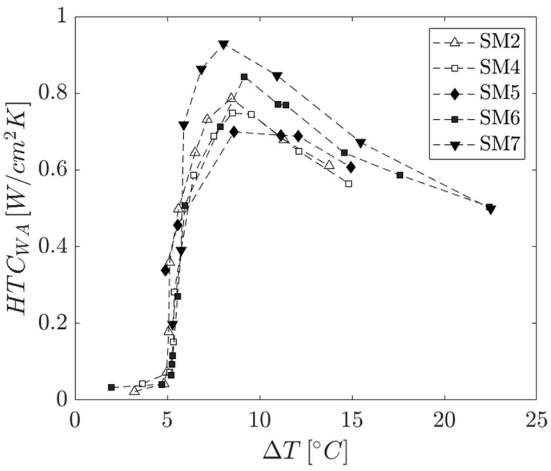

Fig. 6. Heat transfer coefficient calculated with the wetted area as a function of excess temperature for all structured surfaces (SM2-SM7).

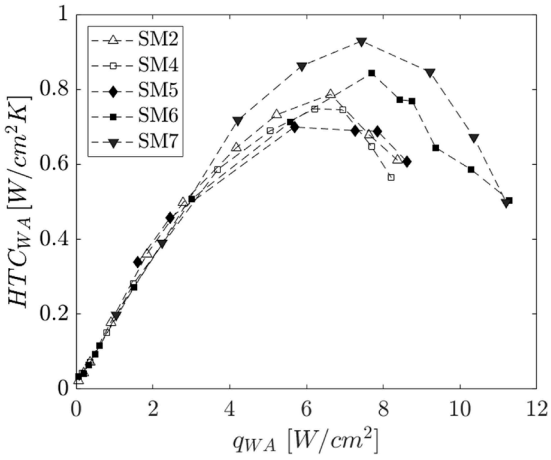

Fig. 7. Heat transfer coefficient as a function of heat flux calculated with the wetted area for all structured surfaces (SM2-SM7).

transfer area from which the same conclusions may be drawn, i.e. the highest fin heat transfer coefficient $HTC_{WA}$is given by the largest spacing between pin fins (SM7).

4.3. The effect of vertical orientation

The effect of surface orientation was also investigated in this study. Experiments with a vertical orientation of the test section have been performed for the smooth (SR1) and two micro-structures samples (SM2 and SM4), see Fig. 8

The smooth sample boiling curve shifts to the left, see Fig. 8(a), showing an earlier onset of nucleation with vertical orientation. The HTC increases from horizontally hot side facing upwards (0°) to vertical (90°) orientations, while the CHF limit is not impacted by the orientation.

The pin-fin structured samples show an opposite effect with the vertical orientation compared to the smooth sample. In fact, the vertical orientation seems to deteriorate the heat transfer and to reduce the CHF limit, as shown by the boiling curves of SM2 and SM4 in Fig. 8(b). The CHF limit reduces 15 % for both the structured samples. The maximum HTC reduces 80 % and 30 % for the SM2 and SM4, respectively. The heat transfer performance reduction with the vertical orientation when using micro-structures has been already observed by previous studies, and ascribed to the difficulty of the bubbles to leave the surface, sliding on walls and merging with other bubbles creating a vapor layer that is not beneficial for heat transfer [33,34].

From the results it can be concluded that operating the heat sink in the vertical orientation might reduce the benefits of adding structures to enhance the heat sink heat transfer performance.

5. Conclusions

This research investigated the enhancement of pool boiling heat transfer of Novec 649 using structured copper surfaces. The structures comprised squared pin fins with varying heights and spacings, machined on the boiling surface using electro-discharge machining (EDM). The dimensions of the pin-fin structures were selected to be close to the fluid's capillary length, ranging from 400 to 1200 μm. The effects of fin height, confinement, and orientation were analysed using a fluid-material combination that remains largely uncharacterised.

The structured samples demonstrated increased values in both the HTC and CHF, outperforming the smooth sample across the entire boiling curve. All fabricated and tested pin fin geometries positively impacted cooling performance compared to smooth surfaces. The largest heat transfer enhancement was achieved with pin fins of 1200 μm height and 400 μm spacing, resulting in a 10-fold increase in HTC and a 2.8-fold increase in CHF compared to the smooth surface. This enhancement is primarily attributed to the increased wetted surface area provided by the fins. The HTC per unit wetted area was found to be independent of geometry during the early stage of nucleate boiling and only weakly

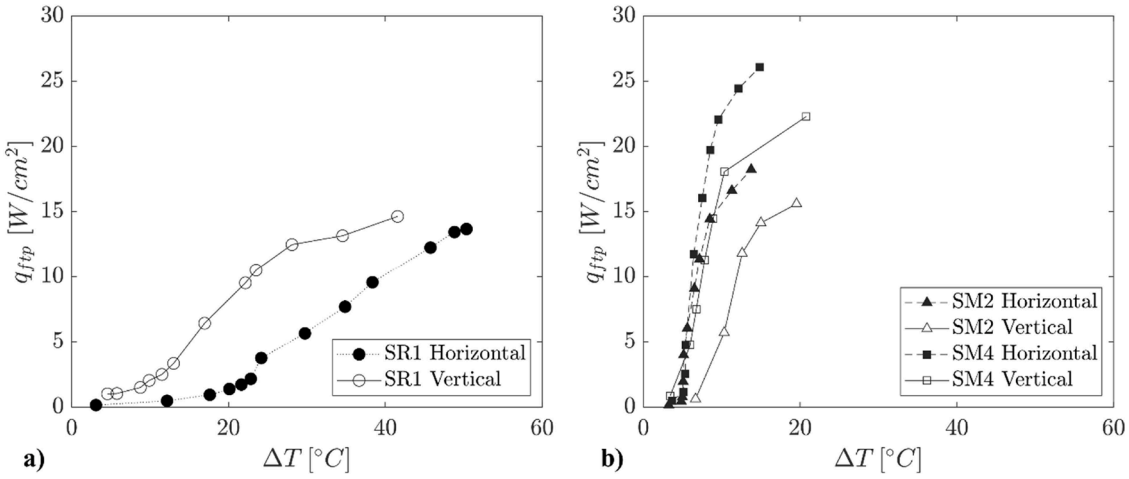

Fig. 8. Boiling curves of (a) the smooth sample (SR1) and (b) structured samples (SM2 and SM4) with horizontal and vertical orientation.

dependent in the latter stages.

The orientation of the boiling surface has a different impact on the heat transfer based on the surface conditions. The structured surfaces show a decrease in performance with the vertical orientation, while the smooth surface shows a slight improvement.

To conclude, within the geometry constraints of this work, the addition of fins to boiling surfaces using Novec 649 provides a promising method to increase heat transfer and CHF from a given footprint. The results of this study support recent findings with FC-72, indicating that the capillary length of the coolant should be considered in the design and optimisation of heat sinks for immersion cooling applications.

CRediT authorship contribution statement

Chiara Falsetti: Writing – review & editing, Writing – original draft, Methodology, Investigation, Funding acquisition, Formal analysis, Data curation, Conceptualization. **Jason Chetwynd-Chatwin:** Resources, Project administration, Investigation, Funding acquisition, Conceptualization. **Edmond J. Walsh:** Writing – review & editing, Methodology, Investigation, Funding acquisition, Formal analysis, Conceptualization.

Declaration of competing interest

The authors declare the following financial interests/personal relationships which may be considered as potential competing interests: Edmond Walsh reports financial support was provided by Rolls-Royce plc.

Data Availability

Data will be made available on request.

References

[1] C. Falsetti, M. Magnini, J.R. Thome, Hydrodynamic and thermal analysis of a micro-pin fin evaporator for on-chip two-phase cooling of high denisty power micro-electronics, Appl. Therm. Eng. 130 (2018) 1425–1439.
[2] R.S. Bartle, E. Walsh, Bubble nucleators to enhance external pool boiling from the bottom row of a tube bundle, Appl. Therm. Eng. 178 (2020).
[3] R.S. Bartle, E. Walsh, Pool boiling of horizontal mini-tubes in unconfined and confined columns, Int. J. of heat and mass transfer," Int. J Heat Mass Transf. 145 (2019) 118733.
[4] R.S. Bartle, K. Menon, E.J. Walsh, Pool boiling of resin-impregnated motor windings geometry, Appl. Therm. Eng. 130 (2018) 854–864.
[5] C. Falsetti, L.R. Amalfi, J. Marcininchen, J.R. Thome, Experimental analysis of the condenser design in a thermosiphon system for cooling of telecommunication electronics, IEEE Trans. Comp. Packag. Manuf. Technol. 10 (2020).
[6] L. Limiao Zhang, C. Wang, G. Su, A. Kossolapov, G. Matana Aguiar, J.H. Seong, F. Chavagnat, B. Phillips, M.M. Rahman, M. Bucci, A unifying criterion of the boiling crisis, Nat. Commun. 14 (2023).
[7] A. Fly, R. Thring, A comparison of evaporative and liquid cooling methods for fuel cell vehicles, Int. J. Hydrogen Energy 41 (2016) 14217.
[8] G. Liang, I. Mudawar, Review of pool boiling enhancement by surface modification, Int. J. Heat Mass Transf. 18 (2019) 892–933.
[9] H. Chua, X. Yu, H. Jiang, D. Wang, N. Xu, Progress in enhanced pool boiling heat transfer on macro- and micro-structured surfaces, Int. J. Heat Mass Transf. 200 (2023) 123530.
[10] S. Singh, D. Sharma, Review of pool boiling and flow boiling heat transfer enhancement through surface modification, Int. J. Heat Mass Transf. 181 (2021).
[11] G. Guglielmini, M. Misale, C. Schenone, Experiments on pool boiling of a dielectric fluid on extended surfaces, Int. Commun. Heat Mass Transf. 24 (1996) 451–462.
[12] K. Rayney, S. You, Pool boiling heat transfer from plain and microporous, square pin-finned surfaces in saturated FC-72, J. Heat Transfer 122 (2000) 509–516.
[13] C. Yu, D. Lu, Pool boiling heat transfer on horizontal rectangular fin array in saturated FC-72, Int. J. Heat Mass Transf. 50 (2007) 3624–3637.
[14] A. Zou, S. Maroo, Critical height of micro/nano structures for pool boiling heat transfer enhancement, Appl. Phys. Lett. 103 (2013) 221602.
[15] S.H. Kim, G.C. Lee, J.Y. Kang, K.K.M.H. Moriyama, Boiling heat transfer and critical heat flux evaluation of the pool boiling on micro structured surface, Int. J. Heat Mass Transf. 91 (2015) 1140–1147.
[16] M.M. Rahman, M. McCarthy, Effect of Length Scales on the boiling enhancement of structured copper surfaces, J. Heat Transfer 139 (2017) 111508.
[17] R. Kaniowski, R. Pastuszko, L. Nowakowski, Effect of geometrical parameters of open microchannel surfaces on pool boiling heat transfer, EPJ Web Conf. 143 (2017).
[18] R. Gouda, M. Pathak, M. Khan, Pool boiling heat transfer enhancement with segmented finned microchannels structured surface, Int. J. Heat Mass Transf. 127 (2018) 39–50.
[19] R. Pastuszko, R. Kaniowski, T. Wojcik, Comparison of pool boiling performance for plain micro-fins and micro-fins with a porous layer, Appl. Therm. Eng. 166 (2020).
[20] R. Kaniowski, R. Pastuszko, Pool boiling experiment with Novec-649 in microchannels for heat flux prediction, Experim. Therm. Fluid Sci. 141 (110802) (2023).
[21] Z. Cao, Z. Wu, B. Sunden, Heat transfer prediction and critical heat flux mechanism for pool boiling of NOVEC-649 on microporous copper surfaces, Int. J. Heat Mass Transf. 141 (2019) 818–834.
[22] Z. Cao, Z. Wu, B. Sunden, Pool boiling of NOVEC-649 on microparticle-coated and nanoparticle-coated surfaces, Heat Transf. Eng. 42 (2021) 19–20.
[23] Z. Lei, B. Liu, P. Xu, Y. Zhang, J. Wei, The pool boiling heat transfer and critical vapor column coalescence mechanism of block-divided microstructured surfaces, Int. J. Heat Mass Transf. 150 (2020).
[24] M. Može, V. Vajc, M. Zupancic, I. Golobic, Hydrophilic and hydrophobic nanostructured copper surfaces for efficient pool boiling heat transfer with water, water/butanol mixtures and Novec 649, Nanomaterials 11 (3216) (2021).
[25] H. Tang, L. Xia, Y. Tang, C. Weng, Z. Hu, X. Wu, Y. Sun, Fabrication and pool boiling performance assessment of microgroove array surfaces with secondary micro-structures for high power applications, Renew. Energy 187 (2022) 790–800.
[26] C. Falsetti, J. Chetwynd-Chatwin, E.J. Walsh, Pool boiling heat transfer of Novec 649 on sandblasted surfaces, Int. J. Thermofluids 22 (100615) (2024).
[27] M. Winter, J. Weibel, The capillary length scale determines the influence of bubble-fin interactions and prediction of pool boiling from heat sinks, Int. J. Heat Mass Transf. 202 (2023) 123727.
[28] M. Zupančič, D. Fontanarosa, M. Može, M. Bucci, M. Vodopivec, B. Nagarajan, M. Vetrano, S. Castagne, I. Golobič, Enhanced nucleate boiling of Novec 649 on thin metal foils via laser-induced periodic surface structures, Appl. Therm. Eng. 236 (2024).
[29] Y. Cengel, A.J. Ghajar, Heat and Mass transfer: Fundamentals and Applications, 5th ed., McGraw-Hill Professional, 2014.
[30] S. Kline, F. McClintock, Describing uncertainties in single-sample experiments, Mech. Eng. 75 (1) (1953) 3–8.
[31] J. Long, Z. Liu, H. Lin, Y. Li, Z. Cao, Z. Zhang, X. Xie, Pool boiling heat transfer and bubble dynamics over V-shaped microchannels and micropyramids: does high aspect ratio always benefit boiling? Appl. Therm. Eng. 201 (2022).
[32] N. Zuber, Hydrodynamic Aspects of Boiling heat Transfer, Doctoral Dissertation of University of California, 1959.
[33] K. Rainey, S. You, Effects of heater size and orientation on pool boiling heat transfer from microporous coated surfaces, Int. J. Heat Mass Transf. 44 (2001) 2589–2599.
[34] K. Rainey, S. You, S. Lee, Effect of pressure, subcooling, and dissolved gas on pool boiling heat transfer from microporous, square pin-finned surfaces in FC-72, Int. J. Heat Mass Transf. 46 (2003) 23–35.